

Scattering in a Coulomb potential: a velocity space point of view

A. González-Villanueva and E. Guillaumin-España

*Laboratorio de Sistemas Dinámicos, Departamento de Ciencias Básicas, Universidad Autónoma Metropolitana-Azcapotzalco
Apartado postal 21-726, 04000 Coyoacán, D.F., Mexico*

H.N. Núñez-Yépez[†]

*Instituto de Física "Luis Rivera Terrazas", Benemérita Universidad Autónoma de Puebla
Apartado postal J-48, 72570 Puebla, Pue., Mexico*

A.L. Salas-Brito[‡]

*Departamento de Física, Facultad de Ciencias, Universidad Nacional Autónoma de México
Apartado postal 21-726, 04000 Coyoacán, D.F., Mexico*

Recibido el 17 de septiembre de 1997; aceptado el 28 de noviembre de 1997

The unbounded motion of a particle in a Coulomb field is analyzed from the point of view of velocity space using both the hodograph and the properties of the Hamilton vector. Many features of the motion even the classical deflection function and the differential scattering cross section *in velocity space* follow from simple geometrical considerations, the standard Rutherford scattering formula in configuration space can then be simply obtained from them. We address the connection between initial conditions and the properties of the scattering orbits with the help of the Hamilton vector. We also discuss an approximate method for calculating the effect of a central perturbation on the properties of the hodograph and on the Rutherford's differential scattering cross section.

Keywords: Classical scattering; Hamilton vector; Keplerian's velocity space

Se analizan los movimientos no confinados de una partícula en un campo coulombiano desde la perspectiva del espacio de las velocidades, empleando para ello a la hodógrafa y algunas propiedades del vector de Hamilton. Muchas características del movimiento, incluyendo tanto a la función de deflexión como a la sección eficaz diferencial *en el espacio de velocidades*, pueden calcularse de consideraciones geométricas simples; la sección usual de Rutherford en el espacio de configuraciones puede obtenerse también muy simplemente de lo anterior. Para finalizar, estudiamos el efecto de un término radial de perturbación sobre las propiedades de la hodógrafa y sobre la sección eficaz de dispersión, empleando para ello una técnica aproximada que aprovecha las propiedades del vector de Hamilton.

Descriptores: Dispersión clásica; vector de Hamilton; espacio de velocidades Kepleriano

PACS: 03.20.+i

1. Introduction

Unbounded orbits of mechanical systems are very important nowadays since they have the leading roles in scattering processes and scattering has become the fundamental tool for the study of many physical phenomena. Perhaps the most basic scattering process of all is scattering in a Coulomb field [1, 2]. One has only to remember the crucial role played by it on establishing the existence of the atomic nucleus and, thus, in shaping the current ideas on the structure of the atom. The enormous interest in atomic, molecular and nuclear collisions have also contributed to the importance of unbounded orbits and to the study of scattering processes in central force fields, which are often used as a first approximation to many interactions.

For obvious reasons then, unbounded orbits in central potentials have been widely studied from the standpoints of both classical and quantum mechanics in the last 85 years or so. Although the study of classical orbits always passes through the study of those of the Coulomb problem, it is a curious fact that they had been seldom discussed from the point of

view of velocity space, using the properties of the hodograph which, at least for the Coulomb problem, is known to produce some simplifying features. As it was probably known by Newton, by Bernoulli and by Laplace, and certainly by Hamilton [3] and by Maxwell [4], the hodograph (*i.e.*, the orbit in velocity space) of the classical Coulomb problem is a circle [5, 6]. This fact might have been known even to Rutherford and could have been used in deriving the famous scattering formula since it was sort of standard in textbooks of the second half of the XIX century [4, 7]. It is a curious fact that this very beautiful result is almost unknown nowadays.

Our point is that, apart from aesthetical considerations, velocity (or momentum) space can be used with profit for describing some features of scattering processes, at least if the outgoing part of the orbits may be described using asymptotes (*i.e.*, when the scattering angle have a simple relationship with the direction of the asymptotic velocity) as is the case of the Coulomb and other related problems. This is a point we will try to make in this article. On the other hand, this appropriateness of velocity space for the study of cen-

tral problems has been well used by Fano and Fano [8] for describing scattering, and by Feynman [9] for discussing the Kepler problem including a derivation of the configuration space Rutherford scattering formula. See also Gutzwiller's book [10] for its relationship with other features of the motion.

The article is organized as follows. In Sect. 2 we derive and discuss the fundamental properties of the Hamilton vector and establish the circularity of the hodograph, next we use such constructs to describe some features of unbounded orbits in the Coulomb problem. In Sect. 3 we employ geometrical considerations on the hodograph to describe a scattering trajectory and next to define and to obtain the differential scattering cross section in velocity space, we then argue how to get Rutherford formula from the differential cross section in velocity space. In Sect. 4 we explore scattering in a centrally perturbed Coulomb field using again the Hamilton vector. Section 5 gives some concluding remarks.

2. The hodograph for the unbounded orbits of the Coulomb problem

The classical Coulomb problem—which is just another name for the Kepler problem when the interaction is regarded as electrostatic instead of gravitational—is a very interesting problem that can be seen from many angles. For example, it is known to be one of the rather limited class of superintegrable problems. This means that there are more than the standard conserved quantities in it; in addition to the energy and the angular momentum, the Hamilton vector can be found as a further constant of motion as it is shown in what follows. The constancy of \mathbf{h} is known to be closely related with the existence of hidden symmetries in the Coulomb problem [11–14].

The equation of motion of two particles with masses m_1 and m_2 interacting through an inverse squared interaction can be, after separating the center of mass motion and introducing the relative coordinate $\mathbf{r} = \mathbf{r}_1 - \mathbf{r}_2$, cast in the form of the equation of motion for a single particle interacting with a centre of force located at the centre of mass of the two original particles where we also assume is located the origin. The mass in this equivalent problem equals the reduced mass of the original particles $m = m_1 m_2 / (m_1 + m_2)$:

$$m \frac{d^2 \mathbf{r}}{dt^2} = \frac{\alpha}{r^2} \hat{\mathbf{e}}_r, \tag{1}$$

where α , \mathbf{r} and $\hat{\mathbf{e}}_r$ are, respectively, a characteristic constant of the interaction, the position vector, and the unit vector in the radial direction. The constant α can be positive, as in the repulsive electrostatic case, or negative, as in the attractive electrostatic or in the gravitational cases. In this work, we are mainly interested in the repulsive case which corresponds to $\alpha > 0$ and hence the motion can be described as scattering.

In the problem described by Eq. (1), the energy E and the angular momentum $\mathbf{L} = m\mathbf{r} \times \mathbf{v}$ are conserved. The conservation of \mathbf{L} is a consequence of the central nature of

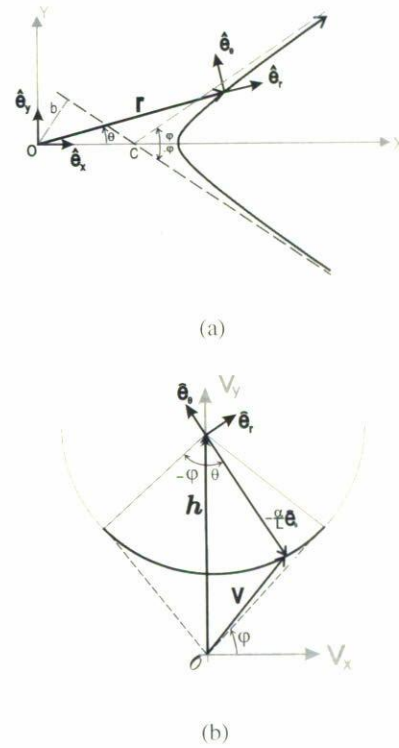


FIGURE 1. The coordinate systems used in the article, cartesian and polar and their corresponding unit vectors, are shown in both the configuration (a) and the velocity (b) spaces; the scattering orbits are also shown as continuous light curves. The centre of force is located at the origin O in configuration space and coincides with the external focus of the hyperbolic path. The incoming and outgoing angles are, respectively, $\varphi = \arccos(1/\epsilon)$ and $-\varphi$, see Eqs. (9) and (10) in the text for the definition of ϵ . The origin in velocity space is labeled O .

the interaction which prevents it from exerting torques upon the scattered particle. It is therefore very easy to see that the motion is confined to the plane orthogonal to \mathbf{L} ; in this orbital plane we may choose a polar coordinate system with unit vectors $\hat{\mathbf{e}}_r$ and $\hat{\mathbf{e}}_\theta$ as illustrated in Fig. 1, where we show a scattering trajectory in both the velocity and the configuration space. We can write the position vector as $\mathbf{r} = r\hat{\mathbf{e}}_r$, hence the velocity \mathbf{v} and the acceleration \mathbf{a} become, respectively,

$$\mathbf{v} = \frac{d\mathbf{r}}{dt} = \dot{r}\hat{\mathbf{e}}_r + r\dot{\theta}\hat{\mathbf{e}}_\theta,$$

and

$$\mathbf{a} = \frac{d\mathbf{v}}{dt} = (\ddot{r} - r\dot{\theta}^2)\hat{\mathbf{e}}_r + (r\ddot{\theta} + 2\dot{r}\dot{\theta})\hat{\mathbf{e}}_\theta, \tag{2}$$

as follow from the polar identities $\dot{\hat{\mathbf{e}}}_r = \dot{\theta}\hat{\mathbf{e}}_\theta$, and $\dot{\hat{\mathbf{e}}}_\theta = -\dot{\theta}\hat{\mathbf{e}}_r$. The angular momentum can also be written as $\mathbf{L} = mr^2\dot{\theta}\hat{\mathbf{e}}_z = L\hat{\mathbf{e}}_z$. These equations allow us to write the equation of motion (1) in the form [6, 7, 15]

$$m\dot{\mathbf{v}} = \frac{\alpha}{r^2}\hat{\mathbf{e}}_r = -\frac{\alpha m}{L}\dot{\hat{\mathbf{e}}}_\theta, \tag{3}$$

providing us immediately with a further conserved quantity, the Hamilton vector

$$\mathbf{h} \equiv \mathbf{v} + \frac{\alpha}{L} \hat{\mathbf{e}}_{\theta}. \quad (4)$$

The magnitude of the Hamilton vector, h , is easily seen to be related with the energy E and with the magnitude of the angular momentum L or with the asymptotic speed at infinity $v_{\infty} = \sqrt{2E/m}$ and L

$$h^2 = \frac{2E}{m} + \frac{\alpha^2}{L^2} = v_{\infty}^2 + \frac{\alpha^2}{L^2}, \quad (5)$$

the last expression can be applied only to the $E > 0$ case since v_{∞} has to be real and shows that when the orbits are unbounded (which is the only possibility if α is assumed positive) h is always greater than v_{∞} .

It is also easy to see that \mathbf{h} is parallel to the velocity at pericentre \mathbf{v}_p [compare with Eq. (9) below], therefore, it can be always written as $\mathbf{v}_p = (h - \alpha/L)\hat{\mathbf{e}}_{\theta}$ or, in other words, that \mathbf{h} points along the *semilatus rectum* in the configuration space orbit [15]. Moreover, as can be seen directly in (4), \mathbf{h} is related with the hodograph of the problem, *i.e.*, with its trajectory in velocity space. Besides, the constancy of the Laplace vector [1, 11, 16], also known as the Runge-Lenz vector, \mathbf{A} , follows as a simple consequence of that of \mathbf{h} and of \mathbf{L}

$$\mathbf{A} = \mathbf{h} \times \mathbf{L} = \mathbf{v} \times \mathbf{L} + \alpha \hat{\mathbf{e}}_r, \quad (6)$$

it should be clear that \mathbf{A} is parallel to the position vector at pericentre as a consequence of \mathbf{h} being parallel to the velocity there [12].

2.1. The scattering hodograph is a circular arc

Equation (4) shows also that, as the motion proceeds, the velocity moves according to the following equation:

$$\mathbf{v} = \mathbf{h} - \frac{\alpha}{L} \hat{\mathbf{e}}_{\theta}, \quad (7)$$

the hodograph of the classical Coulomb problem is thus a circular arc of radius α/L whose centre is at the tip of \mathbf{h} , as illustrated in Fig. 1b. To visualize why it cannot be the complete circle think of the angular range allowed in scattering.

With the help of Eq. (7) the polar components of the velocity are easily seen to be

$$v_r(\theta) = h \sin \theta, \quad (8)$$

and

$$v_{\theta}(\theta) = h \cos \theta - \frac{\alpha}{L}; \quad (9)$$

we can also write down the speed as a function of θ for the scattering orbits

$$v(\theta) = \frac{\alpha}{L} \sqrt{1 + \epsilon^2 - 2\epsilon \cos \theta}, \quad (10)$$

where we defined $\epsilon \equiv hL/\alpha$. Expressions (8) and (9) are the parametric equations of a circle, but notice that according

to Eq. (9) θ can only take values between $-\varphi$ and φ , where the angle φ is defined through $\cos \varphi = 1/\epsilon$, that is, θ must be bounded between the points at which the angular velocity vanishes; as it pertains to a scattering hodograph and since it is just the angle the outgoing velocity makes with the x -axis, the angle φ is called the outgoing angle (see Fig. 1). This corroborates our previous claim that the hodograph is not the complete circle but just an arc. As we will exhibit next, this can only happen if the trajectory in configuration space is unbounded and requires that $\epsilon > 1$. The trajectory in configuration space follows trivially from (9) and the expression for v_{θ} in Eq. (2),

$$r = \frac{p}{\epsilon \cos \theta - 1}, \quad (11)$$

where we introduced the definition $p \equiv L^2/m\alpha$. This is the focal equation of a hyperbola in polar coordinates, p is then the semilatus rectum and ϵ plays the role of the eccentricity; hence, the orbit in configuration space is unbounded. According to (11) the scattering trajectory is the branch of the hyperbola whose external focus coincides with the centre of force (Fig. 1a). Note also that the denominator in Eq. (11) remains positive as long as θ remains confined within the interval mentioned above; hence, its asymptotes make angles φ (outgoing asymptote) and $-\varphi$ (incoming asymptote) with the x -axis. (See again Fig. 1).

As follows from the shadowed triangle depicted in Fig. 2 (see also Sect. 3 below) and from the definition of the eccentricity, the energy can be rewritten in terms of ϵ and h or of ϵ and L , as

$$\begin{aligned} E &= \frac{m}{2} \left(h^2 - \frac{\alpha^2}{L^2} \right) \\ &= \frac{m\alpha^2}{2L^2} (\epsilon^2 - 1); \end{aligned} \quad (12)$$

the condition for unbounded orbits is thus explicitly seen to be $E > 0$ and $\epsilon > 1$.

The previous analysis does not encompass every possible scattering motion, there exist a limiting case requiring a separate analysis: a head-on collision with the centre of force. This is the case of degenerate trajectories with $\mathbf{L} = 0$ where, as follows from (9), the only angle permitted in such a case is $\theta = 0$; therefore, the hyperbolic trajectories degenerate into straight lines. The hodograph also becomes a straight line in this case [5, 6]. As it must be obvious, the constant ϵ can no longer be interpreted as the eccentricity of a conic in the limit of vanishing angular momentum.

2.2. Drawing the hodograph

To draw the hodograph if E and L are known, let us consider a circle with radius v_{∞} centered at the origin and let us call it the reference circle [10]. If the interaction is repulsive, for a given E , and as h is always greater than v_{∞} , every point outside the reference circle determines a possible Hamilton

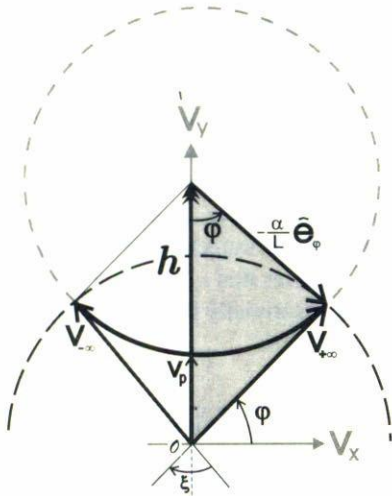


FIGURE 2. The complete hodograph for a scattering orbit in a repulsive Coulomb problem is the dark circular arc shown, the dashed lighter arc is the scattering hodograph with the same values for the energy and the angular momentum but in an attractive field. The centre of the hodograph is at the tip of the Hamilton vector \mathbf{h} , here assumed as in Fig. 1, to point in the positive y -direction. The reference circle of radius $v_\infty = \sqrt{2E/m}$ is shown as a dashed dark arc; the centre of any scattering hodograph should lie outside this reference circle. The vectors $\mathbf{v}_{\pm\infty}$ are tangent to the hodograph, orthogonal to the reference circle and represent the asymptotic values of the velocity at $t = \pm\infty$, besides \mathbf{h} bisects the angle between them. The vector \mathbf{v}_p stands for the velocity at pericentre, ξ is the deflection angle, notice the relationship $\xi/2 + \varphi = \pi/2$. The key for many calculations in the text is either one of the similar right triangles formed by the three vectors \mathbf{h} , $\mathbf{v}_{+\infty}$ and $-\alpha\hat{\mathbf{e}}_\varphi/L$, or by \mathbf{h} , $\mathbf{v}_{-\infty}$ and $-\alpha\hat{\mathbf{e}}_{-\varphi}/L$; $\hat{\mathbf{e}}_\varphi$ and $\hat{\mathbf{e}}_{-\varphi}$ being just $\hat{\mathbf{e}}_\theta$ but evaluated at $\theta = \varphi$ and $\theta = -\varphi$, respectively. One of these fundamental triangles is shadowed for a better identification.

vector which could then be used as the centre of a particular hodograph. Let us select one of these points, *i.e.*, select a value for \mathbf{h} , since this is equivalent to choosing the direction and magnitude of the velocity at pericentre, we are also choosing the orientation of the orbit. From the chosen point draw tangents to the reference circle, the length of any of these tangent lines is the radius of the hodograph, *i.e.*, has the value α/L . The length of the tangents together with their directions give the limiting values of the velocity at $t = \pm\infty$, that is, they give $\mathbf{v}_{\pm\infty}$, therefore the vector $\hat{\mathbf{e}}_\theta\alpha/L$ is orthogonal to $\mathbf{v}_{\pm\infty}$ and the Hamilton vector always bisects the angle between the asymptotic velocities. (See Fig. 2).

Since the reference circle intersects the hodograph, it naturally gets divided into two complementary arcs. The arc inside the reference circle is the hodograph for scattering in a repulsive potential at a certain E and L , this is so since the length of every possible speed in the problem must be less than that of v_∞ . This also makes clear that the point on the hodograph closer to the origin in velocity space corresponds to the pericentre of the orbit in configuration space (but no-

tice that, in the case of an attractive interaction, with $\alpha < 0$, it is the other way round, the pericentre is the point on the hodograph farther from the origin). On the other hand, the complementary arc, outside the reference circle, corresponds to the hodograph for scattering in an attractive potential with the same values of the energy and the angular momentum as in the previous case. This is illustrated in Fig. 2, where we have made \mathbf{h} point along the y -axis. You may also easily see in the figure, or from Eq. (8), that the speed at pericentre is always given by

$$v_p = h - \alpha/L, \tag{13}$$

compare this result with Eq. (23) below. It is important to pinpoint that if we were dealing with an attractive interaction, the speed at pericentre would have had to be given by $v_p = h + \alpha/L$ and not by Eq. (13).

3. The Rutherford scattering formula

3.1. The fundamental triangle in velocity space

In Fig. 2, note any one of the right triangles formed by $\mathbf{v}_{+\infty}$, \mathbf{h} and the vector marked $-\alpha\hat{\mathbf{e}}_\varphi/L$ ($\hat{\mathbf{e}}_\varphi$ is just $\hat{\mathbf{e}}_\theta$ but evaluated at $\theta = \varphi$), or, by $\mathbf{v}_{-\infty}$, \mathbf{h} and the vector marked $-\alpha\hat{\mathbf{e}}_{-\varphi}/L$; in the figure, the first triangle is shadowed. Any one of these triangles together with the relations

$$L = mbv_\infty \quad \text{and} \quad E = mv_\infty^2/2, \tag{14}$$

where b is the *impact parameter* (see Fig. 1a for an illustration), contains all the information needed to calculate the properties of a scattering orbit. For example, the energy Eq. (12) simply follows from Pythagoras theorem applied to the shadowed triangle, and the outgoing angle, φ , can be related to L and v_∞ using simple trigonometry:

$$L = \frac{\alpha}{v_\infty} \tan \varphi, \tag{15}$$

this is the well-known Rutherford relation [1]. On the other hand, notice that such triangle also implies that φ can be alternatively calculated as

$$\varphi = \arctan \left(\frac{2bE}{\alpha} \right). \tag{16}$$

Furthermore, using again Fig. 2, we can see that $\xi/2$ is complementary to φ , thus we get ξ , the deflection angle, as

$$\xi = \pi - 2 \arctan \left(\frac{2bE}{\alpha} \right) = \pi - 2 \arctan \left(\frac{2LE}{mv_\infty\alpha} \right); \tag{17}$$

this is the classical deflection function for the Coulomb problem. From the energy Eq. (12) and the relation $h = \epsilon\alpha/L$, the eccentricity can be rewritten in the form

$$\epsilon = \sqrt{1 + \frac{4b^2 E^2}{\alpha^2}}; \tag{18}$$

this expression shows that a head-on collision (*i.e.*, a collision with $b = 0$) corresponds to $\epsilon = 1$.

3.2. The differential cross section in velocity space

Now, if we are studying scattering in a realistic setting, we have to deal not with a single particle moving in a scattering trajectory but with a whole beam of identical particles following slightly different trajectories. The only assumption usually made in this case is that all the particles in the beam have the same energy and that they come from “infinity” (in practical terms, they come from far away the scattering centre). That is, we have to consider that all the particles have a *common* incoming velocity $\mathbf{v}_{-\infty}$. The particles differ by the values of \mathbf{h} and of \mathbf{L} , trace different hodographs and therefore are scattered through different angles. Notice that all the hodographs traced under these assumptions should be tangent to $\mathbf{v}_{-\infty}$ and therefore that, as we pointed out before, the $\hat{\mathbf{e}}_{\theta}\alpha/L$ vectors associated with them are always orthogonal to the asymptotic velocity. This implies that the Hamilton vectors of every scattering trajectory in the beam have their tips on a line orthogonal—or on a plane, likewise orthogonal, if we take into account the axial symmetry of the scattering problem—to $\mathbf{v}_{-\infty}$. This line (or plane) can be considered also orthogonal to $\mathbf{v}_{+\infty}$ —as can be seen in the fundamental triangles shown in Fig. 2 and in Fig. 3. But be aware that in this last figure, the asymptotic velocity at $\mathbf{v}_{-\infty}$ is *not* oriented in the same direction as the one displayed in Fig. 2 and, though there is no asymptotic velocity explicitly displayed in Fig. 1, it neither corresponds to the case illustrated here.

As the whole scattering process can be assumed to have axial symmetry around $\mathbf{v}_{-\infty}$, it is rather easy to see that every \mathbf{h} associated with a particle in the beam, must lay on a plane orthogonal to the asymptotic incoming velocity; we shall call this plane the *Hamilton plane*. The axial symmetry also implies that the reference circle with radius v_{∞} has to be considered, in the scattering problem under analysis, as a *sphere* with that same radius and centered at the origin in velocity space. Such sphere can be thought of as the locus of every possible outgoing velocity; then, it is important for the calculation we are trying to perform. One has to realize that the Hamilton plane is necessarily tangent to the reference sphere precisely at the tip of $\mathbf{v}_{-\infty}$, as is illustrated in Fig. 4 and, also, although just in a cross section, in Fig. 3.

Note that the whole bunch of scattering hodographs with L fixed form, on turning the system around $\mathbf{v}_{-\infty}$, a torus; the only section of which actually traversed by the particles is *inside* the reference sphere. If we take into account all possible values of L at fixed E , these tori can be seen to pile up inside one another having always as a common point the tip of $\mathbf{v}_{-\infty}$. See Figs. 3 and 4 for schematic illustrations.

To properly describe a scattering process with experimental situations in mind, one needs to evaluate the so-called effective cross section; let us remind the reader that the effective cross section is basically the normalized particle number flux in the beam [1]. We calculate this in the following but, at difference with other treatments and in accordance with the spirit of the article, we evaluate not the configuration space

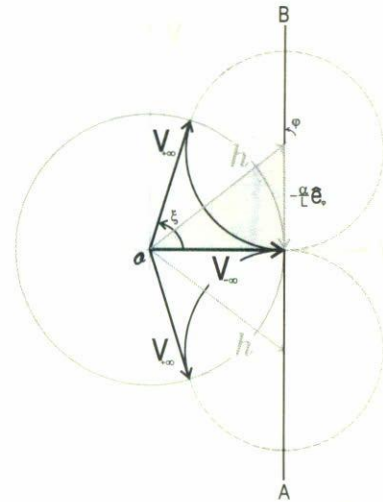


FIGURE 3. Two of the (circular) hodographs in the incident beam of particles are shown together with their common asymptotic incoming velocity $\mathbf{v}_{-\infty}$, here assumed to point in the $+x$ direction—and *not* in the direction shown in Fig. 1. We show two different Hamilton vectors \mathbf{h} and outgoing velocities $\mathbf{v}_{+\infty}$ associated with two of the incoming particles in the beam. Of the whole circles shown, the particles actually traverse just the darkened sections which are inside the reference circle, here shown as a light continuous circle centered at O . The Hamilton plane is shown, just in a section, as the continuous straight line A – B . Given the assumed axial symmetry, on turning this drawing around the x -axis, the hodographs span a nested set of tori (all having $\mathbf{v}_{-\infty}$ as a common point), whereas the Hamilton vectors span a right circular cone whose base lays on the Hamilton plane. See Fig. 4 for a schematic 3D view of this situation.

cross section $d\sigma$ but the *velocity space cross section* $d\Sigma$ and then use the latter to get the former.

Keeping in mind the fundamental triangle referred to in Fig. 3, which on taking into account the axial symmetry becomes the right circular cone, making an angle $\xi/2$ between its generatrix (defined by \mathbf{h}) and its axis (defined by $\mathbf{v}_{-\infty}$), this is shown in Fig. 4. Note that every incoming hodograph (each having the same incoming velocity \mathbf{v}_{∞} and hence the same energy) is characterized by a Hamilton vector $\mathbf{h} = \mathbf{v}_{-\infty} + \hat{\mathbf{e}}_{-\varphi}\alpha/L$ [where $\hat{\mathbf{e}}_{-\varphi} = \hat{\mathbf{e}}_{\theta}(-\infty)$]. Next, let us say that the particles which scatter through angles between ξ and $\xi + d\xi$, have Hamilton vectors between \mathbf{h} and $\mathbf{h} + d\mathbf{h}$; all of these \mathbf{h} 's have their tips laying on the Hamilton plane, but, as the process is axially symmetric around the incoming velocity, the tips of such Hamilton vectors trace on the Hamilton plane an annulus bounded by circles with radii α/L and $\alpha/L + d(\alpha/L)$ —see Eq. (8) and Fig. 4. Thence, the normalized flux of incoming particles or, as we are calling it here, the velocity space cross section $d\Sigma$, is just the area of this annulus:

$$\begin{aligned} d\Sigma &= \left| 2\pi \left(\frac{\alpha}{L} \right) d \left(\frac{\alpha}{L} \right) \right| \\ &= 2\pi \frac{\alpha^2}{L^3} dL; \end{aligned} \quad (19)$$

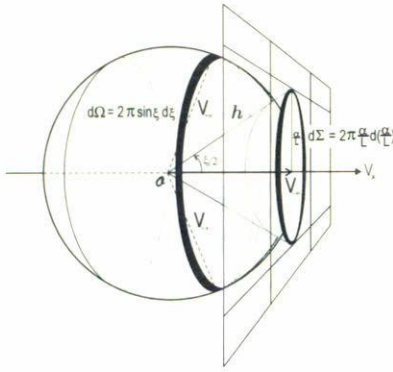


FIGURE 4. The scattering problem seen in a 3D view from velocity space. Of the features mentioned in Fig. 3 and for the sake of clarity, we decided not to show the nested tori. The reference sphere, *i.e.*, the locus of the tips of any possible outgoing velocity for the incoming particles whose Hamilton vectors all lay on the Hamilton plane. This plane just touches (*i.e.*, is tangent to) the reference sphere at the tip of $\mathbf{v}_{-\infty}$. Particles incoming with slightly different Hamilton vectors are represented in velocity space by the gray annulus with radius α/L (*i.e.*, the radius of the hodograph) and width $d(\alpha/L)$ on the Hamilton plane. In configuration space this corresponds to the dark annulus with radius b (b is the impact parameter) and width db shown in Fig. 5. The outgoing particles associated with this section of the incoming beam, corresponds to the annulus with radius $v_{\infty} \sin \xi$ and width $v_{\infty} d\xi$ which lays on the sphere.

the absolute value is necessary since the flux must be positive and thus we need to avoid the minus sign coming from the differential. For comparison with the standard configuration space description take a look at Fig. 5.

As it was to be expected from the start, $d\Sigma$ has the dimensions of an area in velocity space, *i.e.*, it has dimensions of v^2 . If we further consider that all the particles coming in the beam and having Hamilton vectors between \mathbf{h} and $\mathbf{h} + d\mathbf{h}$ (that is, particles in the above mentioned annulus) are scattered through the solid angle $d\Omega = 2\pi \sin \xi d\xi$ in velocity space (which corresponds to the shaded sector on the reference sphere shown in Fig. 4). Thus, the differential scattering cross section *in velocity space* can be evaluated as just the ratio of $d\Sigma$ to $d\Omega$ [1]. In this way we get

$$\frac{d\Sigma}{d\Omega} = \frac{\alpha^2}{L^4} \left| \frac{L}{\sin \xi} \frac{dL}{d\xi} \right|; \tag{20}$$

the absolute value is again necessary for assuring the positivity of the differential cross section. This is the explicit formula for evaluating the differential scattering cross section in velocity space. Notice the similarity of (20) with the standard expression for the differential scattering cross section in configuration space

$$\frac{d\sigma}{d\Omega} = \frac{1}{m^2 v_{\infty}^2} \left| \frac{L}{\sin \xi} \frac{dL}{d\xi} \right|, \tag{21}$$

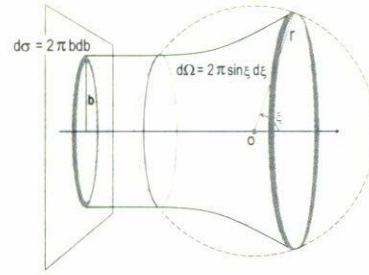


FIGURE 5. The scattering situation from configuration space. We can represent the incoming beam of particles in configuration space as a solid cylinder whose width corresponds to the impact parameter b (which must be regarded in the limit $b \rightarrow \infty$). Particles incoming with slightly different impact parameters are represented by the annulus with radius b and width db . A sphere of radius r is also shown. This standard figure is just shown here for comparison with Fig. 4. We also show two of the scattering trajectories. A derivation of Rutherford cross requires simply taking the ratio of the area of the annulus shown $d\sigma = 2\pi b db$ to the area of the section on the reference sphere $d\Omega = 2\pi \sin \xi d\xi$ to get the standard formula [1] for the differential scattering cross section in configuration space $d\sigma/d\Omega = (b/\sin \xi) |db/d\xi|$.

the main difference being the factor

$$\frac{b^2}{(\alpha/L)^2} = \frac{(L/mv_{\infty})^2}{(\alpha/L)^2} \tag{22}$$

(here expressed in two alternative forms) which transforms the velocity space to the configuration space expression by simply dividing the velocity space cross section by the square of a typical velocity: the radius of the hodograph (constant for each scattering trajectory or hodograph and used in the above derivation of the velocity space cross section) and multiplying it times the square of a typical distance: the impact parameter (also constant for each trajectory or hodograph and used in the corresponding derivation of the configuration space cross section, see, for example Landau and Lifshitz [1] or the caption of Fig. 5). The drawbacks of (20) are the explicit appearance of α and the (related) relationship of its derivation to \mathbf{h} ; formula (20) thus appears to be valid for Coulomb interaction only; though, using the perturbative scheme described in Sect. 4, its range of validity can be extended to centrally perturbed Coulomb interactions.

Using (15) and (17), (20) can be evaluated as

$$\frac{d\Sigma}{d\Omega} = \frac{1}{4} \frac{(\alpha/L)^4}{v_{\infty}^2} \frac{1}{\sin^4 \xi/2} \tag{23}$$

Although correct this expression is not yet totally evaluated because part of the angular dependence is still ‘hidden’ inside of L , it is nevertheless interesting because it expresses the velocity space cross section as a factor which is basically the ratio of two velocity space quantities and because it exhibits the angular dependence of the well-known Rutherford

scattering formula [1, 2]. On using again (17), we finally get

$$\frac{d\Sigma}{d\Omega} = \left(\frac{E}{2m} \right) \frac{1}{\cos^4 \xi/2}; \quad (24)$$

this is Rutherford differential scattering cross section in velocity space.

3.3. Differential cross section in configuration space

It is not simple to put the complete formula (24) to a direct experimental test because scattering experiments are done in configuration space—we just happen to inhabit this and not velocity space and furthermore we are not used to think in terms of it. Multiplying (23) times the dimensional factor (22), we easily get the usual Rutherford expression for the differential scattering cross section in a Coulomb field [1, 2]

$$\frac{d\sigma}{d\Omega} = \frac{(L/mv_\infty)^2}{(\alpha/L)^2} \left(\frac{d\Sigma}{d\Omega} \right) = \left(\frac{\alpha}{4E} \right)^2 \frac{1}{\sin^4 \xi/2}. \quad (25)$$

In the Rutherford scattering formula (25), or in (24), it does not matter whether the interaction is repulsive ($\alpha > 0$), as we have been assuming, or attractive ($\alpha < 0$).

4. Scattering in a perturbed Coulomb field

Many scattering processes cannot be approximated as resulting from interactions with Coulomb-like forces even when the forces are central; then it is of importance to be capable of studying scattering in perturbed Coulomb fields. In this section we exhibit that, even in such a case, the Hamilton vector can still be useful for getting information on the process.

Let us consider then a Coulomb field perturbed by a radial term $\mathbf{f}(r) = f(r)\hat{\mathbf{e}}_r$. With a central perturbation of this sort the equation of motion for the problem reads

$$m \frac{d^2 \mathbf{r}}{dt^2} = \frac{\alpha}{r^2} \hat{\mathbf{e}}_r + \mathbf{f}(r), \quad (26)$$

which illustrates that \mathbf{h} is no longer conserved, its equation of motion becomes [6, 17]

$$\frac{d\mathbf{h}}{dt} = \frac{f(r)}{m} \hat{\mathbf{e}}_r. \quad (27)$$

The velocity, however, can still be expressed in the form

$$\mathbf{v}(t) = \mathbf{h}(t) - \frac{\alpha}{L} \hat{\mathbf{e}}_\theta, \quad (28)$$

in (28), as in (7), the coefficient of $\hat{\mathbf{e}}_\theta$ is a constant whereas the Hamilton vector is now a quantity whose time evolution is determined by (27) and (26). Although we cannot give explicitly the shape of the hodograph for the general case unless we first give $\mathbf{f}(r)$ and then solve Eq. (27), we can, at least, evaluate some of its geometrical properties. For example, let us compute the hodograph's curvature in velocity space [18], using the definition of curvature and keeping in mind that the hodograph's arc-length is just the speed v , we easily get

$$\mathbf{K}_h = \frac{d\mathbf{v}}{dv} = \frac{1}{a} \frac{d\mathbf{v}}{dt} = \frac{L/\alpha}{1 + r^2 f(r)/\alpha} \hat{\mathbf{e}}_\theta; \quad (29)$$

from here, the hodograph's radius of curvature follows immediately as

$$R_h = \frac{\alpha}{L} (1 + f(r)r^2/\alpha). \quad (30)$$

This is as far as we want to get without an explicit expression for $f(r)$. But, it is easy to obtain further information if we allow for approximations, as we show next.

Let us note that Eq. (27) can be at least formally solved to obtain the change in \mathbf{h} due to the perturbation

$$\Delta \mathbf{h} = \frac{1}{m} \int_{-\infty}^{+\infty} f(r(t)) \hat{\mathbf{e}}_r dt, \quad (31)$$

the only disadvantage of this equation is that the integration must incorporate the solution to Eq. (26). It is usually more useful to express the integration in (31) in terms of θ using angular momentum conservation, so

$$\Delta \mathbf{h} = \frac{1}{L} \int_{\varphi_i}^{\varphi_o} r(\theta)^2 f(r(\theta)) \hat{\mathbf{e}}_r d\theta, \quad (32)$$

where φ_o and φ_i are, respectively, the incoming and the outgoing angles in the perturbed problem. If we further assume that the perturbation is small, it becomes valid to approximate (32) by evaluating it along the unperturbed trajectory; then, noting the integrand's parity, coming in part from $\hat{\mathbf{e}}_r = \hat{\mathbf{e}}_x \cos \theta + \hat{\mathbf{e}}_y \sin \theta$, we get

$$\delta \mathbf{h} = \frac{\hat{\mathbf{e}}_x}{L} \int_{-\varphi_c}^{\varphi_c} r_c(\theta)^2 f(r_c(\theta)) \cos \theta d\theta, \quad (33)$$

where φ_c stands for the asymptotic angle in the unperturbed Coulomb problem given in (16). In fact, we are using a subscript c in every quantity evaluated on the unperturbed trajectory and we use δ , instead of Δ , to indicate the approximation made (*i.e.*, the use of δ means, for example, $\delta \mathbf{h} \simeq \Delta \mathbf{h}$). Note that Eq. (33) says that, if the perturbation is small, the net change in \mathbf{h} occurs in the x -direction, *i.e.*, it is orthogonal to \mathbf{h} and has very little effect on its magnitude. Hence, we can visualize the effect of the perturbation as a clockwise rotation in the orbital plane (in the case of an attractive interaction the rotation is counterclockwise) of the unperturbed hodograph by the angle

$$\delta \varphi = \frac{\delta h}{h} = \frac{1}{hL} \int_{-\varphi_c}^{\varphi_c} r_c(\theta)^2 f(r_c(\theta)) \cos \theta d\theta, \quad (34)$$

where we have made the approximation $\tan \delta \varphi \simeq \delta \varphi$ (valid since we are assuming $\delta \varphi \ll 1$) and where $r_c(\theta)$ must be taken from Eq. (11). Thus the hodograph in the perturbed Coulomb problem can be imagined as an interpolating curve between the circular arcs of two Coulomb-like hodographs whose centers are displaced $\delta \mathbf{h}$ as is illustrated schematically in Fig. 6.

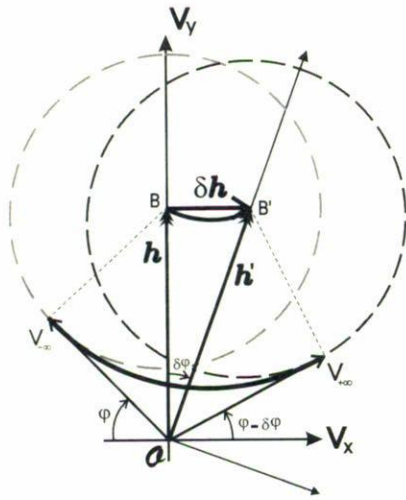


FIGURE 6. Schematic representation of the hodograph of a scattering orbit in the perturbed Coulomb problem. To draw the hodograph it is assumed that the perturbation is small, so the net effect is similar to a small shift of the unperturbed hodograph centre by δh ; the original and the displaced hodographs are shown as thin dashed lines. The perturbed hodograph is a sort of interpolating curve between them. The dark curve from B to B' represents schematically the trajectory of \mathbf{h} during the motion. The magnitude of the change in the outgoing angle is $\delta\varphi$.

With these results, it becomes easy to obtain the deflection function for the perturbed Coulomb problem. As we can see in Fig. 6, the deflection angle changes by $\delta\xi = \delta\varphi$ (at least if we assume that L and E do not change respect the unperturbed case) and thus the deflection angle in the perturbed problem, ξ , can be written as

$$\xi = \xi_c + \delta\xi = \pi - 2 \arctan\left(\frac{2bE}{\alpha}\right) + \frac{1}{hL} \int_{-\varphi_c}^{\varphi_c} r_c(\theta)^2 f(r_c(\theta)) \cos\theta \, d\theta. \quad (35)$$

With this result it is possible to correct the Rutherford scattering cross section for the effect of the perturbing term; to this end we can use as starting points any one of the expressions (20), (21), or even the more explicit Rutherford formulas (24) or (25). But, given the standard use of Rutherford expression in configuration space, we have decided to derive the correction starting from (25). So, using $\xi/2 + \delta\xi/2$ instead of $\xi/2$ as argument of the sine in (25), expanding the resulting expression in powers of $\delta\xi$, and after a straightforward if a bit boring calculation, we obtain the approximate scattering cross section (to first order in $\delta\xi$) in the perturbed problem as

$$\left(\frac{d\sigma}{d\Omega}\right) = \left| \left(\frac{d\sigma}{d\Omega}\right)_c + \delta \left(\frac{d\sigma}{d\Omega}\right) \right|, \quad (36)$$

which is the Rutherford cross section $(d\sigma/d\Omega)_c$, given in Eq. (25), plus the correction term

$$\delta \left(\frac{d\sigma}{d\Omega}\right) = -4 \frac{\delta h}{h} \left(1 + \frac{\alpha}{2bE} + \left(\frac{\alpha}{2bE}\right)^2 \right) \left(\frac{d\sigma}{d\Omega}\right)_c. \quad (37)$$

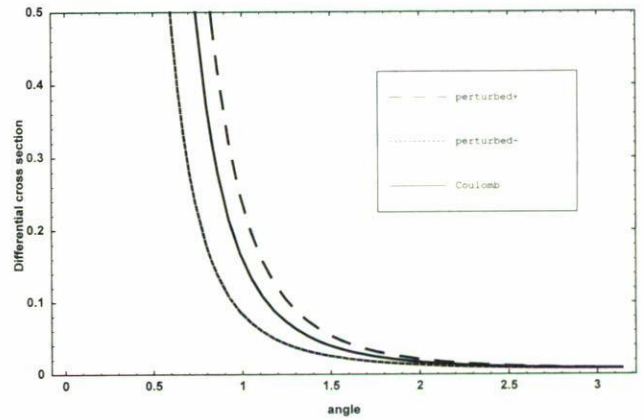


FIGURE 7. Plots of the differential scattering cross sections of the unperturbed Coulomb (solid line) together with the Coulomb perturbed by a β/r^3 term with $\beta > 0$ (dashed line, labeled perturbed+) and $\beta < 0$ (finely dashed line, labeled perturbed-) against the deflection angle between 0 and π . As you can see, under a small repulsive perturbation the cross section diminishes respect the pure Coulomb case and increases if the perturbation is attractive. In the plotting, the values $\alpha = 1$, $\beta = \pm 0.025$, $m = 1$ and $E = 2$, in arbitrary units, were used.

We can, using Eq. (17), express the change in the differential cross section in terms of ξ , in this form we finally get the rather general expression

$$\delta \left(\frac{d\sigma}{d\Omega}\right) = -4\delta\xi \left(\csc^2 \xi/2 + \cot \xi/2 \right) \left(\frac{d\sigma}{d\Omega}\right)_c. \quad (38)$$

for the differential scattering cross section. Thus, we only need to evaluate (34) with the chosen perturbation to be able to get the perturbed differential scattering cross section in this approximation. Let us pinpoint that, starting from (20) or from (24), an expression analogous to (38) for the differential scattering cross section in velocity space can be obtained; although perhaps the easiest way to do this is simply to multiply (38) times the dimensional factor (22).

For perturbing terms of the form $f(r) = \beta/r^s$, where β and s are constants, a general expression for $\delta\xi$ is rather easy to obtain; however, such expression is cumbersome and offers little insight. Thus we have decided that, as an example, it is much better to write down explicitly $\delta\xi$ for the specific perturbing field: β/r^3 . With the perturbation just mentioned the integral (34) is elementary and it is rather easy to get

$$\delta\xi = E \frac{\beta}{\alpha^2} \frac{(\pi - \xi - \sin \xi)}{\cot^2 \xi/2}, \quad (39)$$

An analysis of Eqs. (38) and (39) exhibit that the scattering cross section decreases if the perturbation is repulsive ($\beta > 0$) and increases if the perturbation is attractive ($\beta < 0$) as Fig. 7 illustrates. Equation (38) shows how the Hamilton vector and the hodograph are useful even in this approximate approach, since the change in the scattering cross section can

be written in terms the relative change in h . The results obtained in this section, can be shown to be rather succesful on comparing with several known results, some details of the discussion can be found in González-Villanueva *et al.* [6] and in Aguiar and Barroso [19].

Keep in mind though that the above results are just an approximation to the process valid if the perturbation $f(r)$ is reasonably small and if it makes sense describing the outgoing motion as following asymptotes. Under such conditions, and if the perturbation is repulsive, *i.e.*, if $f(r) > 0$, it is easy to see that the deflection angle of the scattered particle decreases; namely, the outgoing asymptote rotates by the angle $-\delta\xi$; if, on the other hand, the perturbation is attractive, the deflection angle increases by $\delta\xi$.

5. Concluding remarks

We have shown how the scattering orbits in the Coulomb problem can be understood using the Hamilton vector \mathbf{h} . This constant of motion is rather important since, besides being related with the hidden symmetries and superintegrability properties of the problem [11, 12, 14], allows a very simple solution to it. On the other hand, we have exhibited that \mathbf{h} not only determines the spatial orientation but can easily convey other geometric features of the orbit. The hodograph of the problem is closely related with \mathbf{h} and, as we have exhibited in this article, they both suffice to solve the problem and to get the angular dependence of the differential scattering cross section in a Coulomb field. We have shown also how the scattering problem can be discussed from the point of view of velocity space and have obtained an expression for the differential scattering cross section in that space.

Furthermore, we have shown that, taking advantage of the properties of \mathbf{h} , we can obtain some basic geometric information about the hodograph of even a perturbed Coulomb problem. We have also discussed how the Hamilton vector may offer a general framework for studying classical scattering in such perturbed case in an approximate fashion. The complete analysis of specific examples is beyond the scope of this paper, but you can consult, for example, [6] where the deflection angle for the exactly solvable perturbation β/r^3 is calculated and compared with the result obtained using the approximate scheme described here. A related approach to scattering in a perturbed Coulomb field with examples can be found in the article of Aguiar and Barroso [19]. But they use the Laplace vector instead of Hamilton's in the discussion and do not touch on the use of the hodograph for discussing the problem nor on studying the scattering problem from the point of view of velocity space.

Acknowledgments

This work has been partially supported by CONACyT (grant 1343P-E9607) and is dedicated to our late friends M. Mina, M. Gluckhen, M. Mizton, G. Candelita, B. Minina, Q. Motita and M. Miztli. We want to thank also the Fundación Ricardo J Zevada for contributing the software with which the graphics were done. In revising the typescript the help and the useful comments of U. Ek, K. Quiti, T. Rayita, M. Billi and G. Tigga were extremely useful and are gratefully acknowledged. Last but not least, AGV wants to acknowledge with thanks Luis González y González and Armida de la Vara for all the academic support and encouragement given to him.

-
- †. On sabbatical leave from Departamento de Física, UAM-Iztapalapa.
 - ‡. On sabbatical leave from Laboratorio de Sistemas Dinámicos, Departamento de Ciencias Básicas, UAM-Azcapotzalco.
 - 1. L. Landau and E.M. Lifshitz, *Mechanics*, (Pergamon, Oxford, 1976), Chap. IV.
 - 2. L. Landau and E.M. Lifshitz, *Quantum Mechanics*, (Pergamon, Oxford, 1977), §135.
 - 3. W.R. Hamilton, *Proc. Roy. Irish Acad.* **3** (1846) 344.
 - 4. J.C. Maxwell, *Matter and motion*, (Dover, New York, 1952), p. 107. Originally printed in 1877.
 - 5. A. González-Villanueva, H.N. Núñez-Yépez, and A.L. Salas-Brito, *Eur. J. Phys.* **17** (1996) 168.
 - 6. A. González-Villanueva, H.N. Núñez-Yépez, and A.L. Salas-Brito, *Rev. Mex. Fis.* **44** (1997).
 - 7. W. Thomson and P.G. Tait, *Treatise on Natural Philosophy*, (1962 reprint) (Dover, New York, 1962), §37-§38. Originally printed in 1879.
 - 8. U. Fano and L. Fano, *Basic Physics of Atoms and Molecules*, (Wiley, New York, 1958), Appendix III.
 - 9. D.L. Goodstein and J.R. Goodstein, *Feynman's lost lecture, the motion of planets around the sun*, (Norton, New York, 1996), Chap. 4.
 - 10. M.C. Gutzwiller, *Chaos in classical and quantum mechanics*, (Springer, New York, 1990) §12.4.
 - 11. R.P. Martínez-y-Romero, H.N. Núñez-Yépez, and A. L. Salas-Brito, *Eur. J. Phys.* **13** (1992) 26.
 - 12. R.P. Martínez-y-Romero, H.N. Núñez-Yépez, and A.L. Salas-Brito, *Eur. J. Phys.* **14** (1993) 71.
 - 13. O. Campuzano-Cardona, H.N. Núñez-Yépez, A.L. Salas-Brito, and G.I. Sánchez-Ortiz, *Eur. J. Phys.* **16** (1995) 220.
 - 14. A.L. Salas-Brito, H.N. Núñez-Yépez, and R.P. Martínez-y-Romero, *Intl. J. Mod. Phys. A* **12** (1997) 271.
 - 15. D. Moreno, *Gravitación Newtoniana*, FCUNAM, México City (1990).
 - 16. V.I. Arnold, *Mathematical Methods of Classical Mechanics*, (Springer, New York, 1978).
 - 17. J. Sivardière, *Eur. J. Phys.* **13** (1992) 64.
 - 18. J. McCleary, *Geometry from a differentiable viewpoint*, (Cambridge University Press, Cambridge, 1994) Chap. 7.
 - 19. C.E. Aguiar and M.F. Barroso, *Am. J. Phys.* **64** (1996) 1042.